

EXACT LAGRANGIAN FILLABILITY OF 3-BRAID CLOSURES

JAMES HUGHES AND JIAJIE MA

ABSTRACT. We determine when a Legendrian quasipositive 3-braid closure in standard contact \mathbb{R}^3 admits an orientable or non-orientable exact Lagrangian filling. Our main result provides evidence for the orientable fillability conjecture of Hayden and Sabloff, showing that a 3-braid closure is orientably exact Lagrangian fillable if and only if it is quasipositive and the HOMFLY bound on its maximum Thurston-Bennequin number is sharp. Of possible independent interest, we construct explicit Legendrian representatives of quasipositive 3-braid closures with maximum Thurston-Bennequin number.

1. INTRODUCTION

Legendrian links and their exact Lagrangian fillings are central to the study of low-dimensional contact and symplectic topology [Cha10, HS15, BST15]. Following earlier works [EHK16, Pan17, STZ17, STWZ19], recent developments have significantly advanced the construction and classification of orientable exact Lagrangian fillings of Legendrian links in the standard contact \mathbb{R}^3 [CG22, CZ21, ABL22, Hug23b, CN22, CW22, CGG⁺25, CG24], especially for 0- and (-1) -framed closures of positive braids; see Figure 2 for corresponding Legendrian representatives. Concurrently, the study of non-orientable exact Lagrangian fillings has increasingly emerged as a companion to these advances [CCPR⁺23, CSC23, CSHW25]. While the works cited above represent significant progress towards understanding exact Lagrangian fillings for certain families of Legendrian links, it is not yet known exactly which smooth link types have Legendrian representatives in \mathbb{R}^3 with exact Lagrangian fillings, orientable or not. Such a link is termed **orientably** or **nonorientably exact Lagrangian fillable** respectively.

Orientable fillability is closely related to the hierarchy of positivity in smooth knot theory. In particular, [BO01] and [Eli95] together imply that an orientably fillable link is at least quasipositive, and being positive [HS15]—or almost positive in some cases [Tag19]—is a sufficient condition for fillability.¹ However, not all (strongly) quasipositive links are orientably fillable [HS15]. Another necessary condition for orientable fillability is that the HOMFLY polynomial bound on the maximum Thurston-Bennequin number of an orientably fillable link must be sharp [HS15]; see Section 2.2. Hayden and Sabloff conjectured that this condition together with quasipositivity characterizes all orientably fillable links [HS15, Conjecture 1.3].

In comparison, non-orientable fillability is more subtle. On one hand, the Kauffman polynomial bound on the maximum Thurston-Bennequin number of a non-orientably fillable link is sharp [CCPR⁺23], providing an analogue of the HOMFLY bound appearing in the orientable case. On the other hand, the relationship between non-orientable fillability and the positivity hierarchy is more obscure and no conjecture exists about sufficient conditions for non-orientable fillability. While positive links are not decomposably non-orientably fillable, there are links that realize every combination of quasipositivity and non-orientable fillability, and not all negative links are non-orientably fillable [CCPR⁺23]. There are also examples of non-orientably fillable knots that are neither quasipositive nor negative [CCPR⁺23].

2020 *Mathematics Subject Classification.* 53D12; 53D10.

¹For some families of knots, positivity is also a necessary condition for orientable fillability; see [LS19] for the case of 4-plat links.

In this paper, we answer the exact Lagrangian fillability problem for (0-framed) closures of quasipositive 3-braids. Combined with previous results, it gives a complete orientable fillability classification of closures of 3-braids. Let $\hat{\beta}$ be the smooth 0-framed closure of a braid $\beta \in \text{Br}_3$. Denote by $\Delta = \sigma_1\sigma_2\sigma_1$ the Garside element of Br_3 . Using the Garside normal form of β , up to conjugation, we can write

$$(1) \quad \beta = \sigma_1^{k_1} \sigma_2^{k_2} \dots \sigma_1^{k_{r-1}} \sigma_2^{k_r} \Delta^m,$$

where $k_r = 0$ if and only if m is odd, and otherwise $k_i \geq 2$ for all i . Further, m is uniquely determined in this form; see Section 2.1 for more details. The following result characterizes orientable fillability of $\hat{\beta}$.

Theorem 1.1. *The closure $\hat{\beta}$ of a 3-braid β is orientably exact Lagrangian fillable if and only if β is quasipositive and $m \geq -2$.*

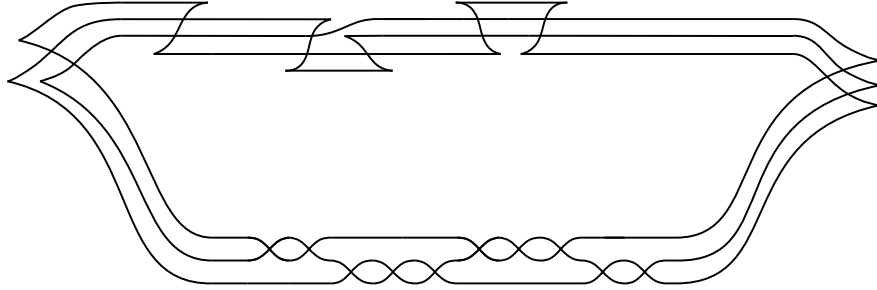


FIGURE 1. Max-tb Legendrian representative of the closure of $\sigma_1^3\sigma_2^2\sigma_1^2\sigma_2^2\sigma_1^3\sigma_2^3\sigma_1^2\Delta^{-7}$. This knot has no orientable exact Lagrangian fillings, but is non-orientably fillable.

By our discussion above, it suffices to consider the case when $\hat{\beta}$ is quasipositive and $m \leq -1$. The case when $m = -1$ is covered in [CGG⁺25, Section 4.3]. For $m \leq -1$, we exploit Orevkov's characterization [Ore04] of quasipositive 3-braids to provide explicit max-tb Legendrian representatives $\Lambda(\beta)$ of $\hat{\beta}$; see Figure 1 for an example. As rainbow closures of positive braids are max-tb Legendrian representatives, our construction allows us to characterize the maximum Thurston-Bennequin number of all quasipositive 3-braids. In more detail, we have the following corollary:

Corollary 1.2. *Let $\hat{\beta}$ be the closure of a quasipositive 3-braid of β of the form given in Equation 1. The maximum Thurston-Bennequin number of $\hat{\beta}$ is given by*

$$\overline{\text{tb}}(\hat{\beta}) = \begin{cases} |\beta| - 3 & m \geq -1, \\ |\beta| + m - 1 & m \leq -2, \end{cases}$$

where $|\beta|$ is the signed word length of β .

When $m = -2$, we construct a decomposable orientable exact Lagrangian filling of $\Lambda(\beta)$. When $m < -2$, we use $\Lambda(\beta)$ to prove explicitly that the HOMFLY polynomial bound on $\overline{\text{tb}}(\hat{\beta})$ is not sharp and thus, $\hat{\beta}$ is not orientably fillable.

Notably, when m is even and less than -2 , our construction of $\Lambda(\beta)$ yields examples of non-fillable max-tb representatives with rotation number equal to zero.

Corollary 1.3. *There exist quasipositive max-tb Legendrian links with rotation number 0 that do not admit any orientable fillings.*

Nonzero rotation number obstructs orientable fillability [Cha10], and to our knowledge, these are the first known examples where this obstruction vanishes but the HOMFLY bound is not sharp. A direct

search of all quasipositive knots with 11 or fewer crossings via KnotInfo [LM25] reveals only one example, namely $m(10_{155})$, which can be realized as the closure of the braid $\beta = \sigma_1^3 \sigma_2^2 \sigma_1^2 \sigma_2^3 \sigma_1^2 \sigma_2^2 \Delta^{-4}$.

As another corollary of Theorem 1.1, our result supports the Hayden-Sabloff conjecture.

Corollary 1.4. *The Hayden-Sabloff fillability conjecture holds for links of braid index 3. Namely, every orientably fillable 3-braid closure is quasipositive and has sharp HOMFLY bound.*

Remark 1.5. One might hope to extend our methods above to characterize orientable fillability of links with higher braid index. The primary difficulty is that we rely heavily on Orevkov’s characterization of quasipositivity for 3-braids; no such characterization is known for higher braid index. To our knowledge [Ore15] represents the furthest progress towards understanding the case of 4-braids.

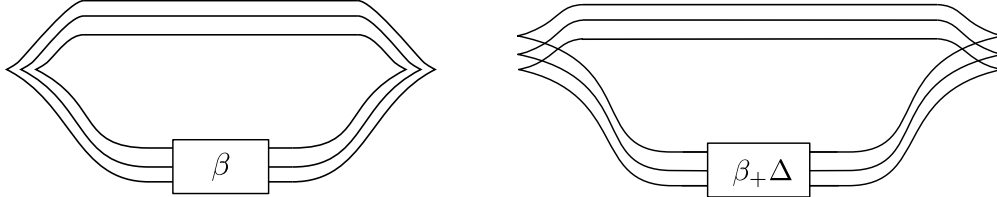


FIGURE 2. Rainbow closure of a positive braid β (left) and (-1) -closure of $\beta_+ \Delta$ (right).

In the context of the recent work on the construction and classification of exact Lagrangian fillings of (-1) -closures of certain families of positive braids cited earlier, we wish to note that every orientably fillable max-tb representative we construct using our method is the (-1) -closure of a positive braid; see Figure 2 (right) for a (-1) closure of $\beta_+ \Delta$. To our knowledge, this is true of all existing examples of orientably fillable Legendrian links, including the ones studied in this paper, suggesting the following question:

Question 1.6. *Do there exist orientably fillable Legendrian links that are not (-1) -closures of positive braids?*

This question has implications for the construction of Lagrangian fillings, as the method of Legendrian weaves, introduced for 2-braids in [TZ18] and generalized to higher braid index in [CZ21], requires that the boundary link be given as the (-1) -closure of a positive braid. This method involves constructing Legendrian surfaces by combinatorially representing a certain class of Legendrian wavefront singularities, and taking the Lagrangian projection of the resulting Legendrian surface to obtain an exact Lagrangian filling. Answering Question 1.6 in the negative would leave open the possibility that every orientably fillable Legendrian admits an exact Lagrangian filling constructed as a Legendrian weave. A careful analysis of the fillings we construct in Section 4 reveals that this is the case for the fillings we construct in this work.

Corollary 1.7. *Every orientably fillable 3-braid closure has at least one max-tb representative that admits an exact Lagrangian filling obtained as the Lagrangian projection of a Legendrian weave.*

We believe that Corollary 1.7 is of possible interest because Legendrian weaves provide a powerful tool for constructing and distinguishing exact Lagrangian fillings. Weaves are currently the best way of identifying what are known as \mathbb{L} -compressing cycles of a filling L , i.e. elements of $H_1(L)$ that bound Lagrangian disks in the complement $\mathbb{B}^4 \setminus L$. These cycles are crucial ingredients in describing cluster structures coming from sheaf-theoretic or Floer-theoretic invariants of Legendrian links. From a cluster-theoretic perspective, the class of 3-braid closures is of particular interest as it contains the smallest known examples of Legendrians with augmentation varieties with multiple irreducible components; see [LN24, Section 2.2.2] for an explicit computation. We hope to further

explore the construction and classification of fillings of the orientably fillable Legendrian links identified here in future work.

Our next result concerns non-orientable fillability of quasipositive 3-braids.

Theorem 1.8. *The closure $\hat{\beta}$ of a quasipositive 3-braid β is non-orientably exact Lagrangian fillable if $m \leq -2$. If $m \geq -1$, then $\hat{\beta}$ does not admit any decomposable non-orientable exact Lagrangian fillings.*

See Section 2.4 for the definition of decomposable. The case when $m \geq 0$ is proven in [CCPR⁺23] using a normal ruling obstruction. We apply the same technique to the case $m = -1$. For $m \leq -2$, we construct a decomposable non-orientable exact Lagrangian filling of the max-tb Legendrian representative $\Lambda(\beta)$ based on a normal ruling. In contrast with Theorem 1.1, Theorem 1.8 does not cover all non-orientably fillable Legendrians of braid index 3 due to the fact that, as mentioned above, our methods rely on the quasipositivity characterization of [Ore04]. In particular, there are known examples, such as the figure-eight knot, of 3-braid closures that are not quasipositive and are non-orientably fillable. Note that the case of $m = -2$ provides a new family of examples of Legendrian links that admit both orientable and non-orientable fillings, behavior originally observed in [CCPR⁺23].

Remark 1.9. While we only construct a single non-orientable filling for each Legendrian in our proof of Theorem 1.8, we expect that a similar approach could produce a collection of (possibly distinct) fillings. One could reasonably hope to apply cluster theoretic methods similar to those used in [CSHW25] to distinguish them by their induced (ungraded) augmentations of the Legendrian contact dg-algebra.

The remainder of this paper is organized as follows: We review background on quasipositive 3-braids, on Legendrian links and their ruling invariants, and on constructions and obstructions of exact Lagrangian fillings of Legendrian links in Section 2. In Section 3, we describe the max-tb Legendrian representatives of quasipositive 3-braid closures touched above and associate with them a ruling. We prove Theorem 1.1 in Section 4 and Theorem 1.8 in Section 5.

Acknowledgments. We thank Lenny Ng for helpful advice and feedback throughout this project. We also thank Josh Sabloff for the question that led us to consider non-orientable fillability and for discussing his conjecture with us. Zijun Li was involved in an earlier version of this project and we are grateful for his contribution.

2. BACKGROUND

2.1. Quasipositive 3-braids. Let Br_3 denote the 3-stranded braid group generated by σ_1, σ_2 , where σ_i corresponds to a single positive crossing between strands i and $i + 1$ of the braid, subject to the Artin relation $\sigma_1\sigma_2\sigma_1 = \sigma_2\sigma_1\sigma_2$. Denote by Br_3^+ the submonoid of Br_3 generated by σ_1 and σ_2 . Also, let $\Delta = \sigma_1\sigma_2\sigma_1$ denote the half-twist on 3 strands, i.e. the **Garside element** of Br_3 . Then, any element $\beta \in \text{Br}_3$ can be written in the **Garside normal form**

$$\beta = \beta_+ \Delta^m,$$

for some $m \in \mathbb{Z}$ and $\beta_+ \in \text{Br}_3^+$ does not contain any power of Δ . This presentation is unique up to the Artin relation by [Ore04, Corollary 2.3].

We say that a braid β is **positive** if it is in Br_3^+ and **quasipositive** if $\beta = \prod_j a_j x_j a_j^{-1}$ for $a_j \in \text{Br}_3$ and $x_j \in \text{Br}_3^+$. Observe that a positive braid is necessarily quasipositive. These notions of positivity can be equivalently stated using the Garside normal form. First, note that β is positive if and only if $m \geq 0$. For $m < 0$, the following criterion of quasipositivity is due to Orevkov.

Theorem 2.1 ([Ore04], Proposition 3.1). *Let $\beta = \beta_+ \Delta^m$ where $\beta_+ \in \text{Br}_3^+$ and $m \leq 0$. The braid β is quasipositive if and only if one can delete letters from β_+ so that the obtained word is equal in Br_3^+ to the word Δ^{-m} .*

We will consider the (0–framed) closure $\hat{\beta}$ of a braid $\beta \in \text{Br}_3$, whose smooth isotopy class is characterized by β up to not only the Artin relations but also conjugation. In this setting, we can conjugate the Garside normal form of β and write more concretely

$$\beta = \sigma_1^{k_1} \sigma_2^{k_2} \dots \sigma_1^{k_{r-1}} \sigma_2^{k_r} \Delta^m,$$

where $k_r = 0$ if and only if m is odd, and otherwise $k_i \geq 2$ for all i . Using the uniqueness of Garside normal form in Br_3 , it is not hard to see that m is uniquely determined to be greatest among all braid words realizing the knot type $\hat{\beta}$. In particular, conjugating β in the form of Equation 1 does not increase m .

A smooth link is **positive** if it has a projection in which all crossings are positive. However, not all positive links are closures of positive braids; see, for example, [Hed] and references therein. On the other hand, a link is **quasipositive** if it is the closure of a quasipositive braid. Note that there is no ambiguity in this definition: if $\beta = \prod_j a_j x_j a_j^{-1}$ is a quasipositive braid, observe that the conjugate $\alpha \beta \alpha^{-1}$ is still quasipositive by inserting $\alpha \alpha^{-1}$ or $\alpha^{-1} \alpha$ in between the products $a_j x_j a_j^{-1}$. Thus, $\hat{\beta}$ is quasipositive as a smooth link if and only if β is quasipositive as a braid. In terms of Equation 1, Orevkov’s characterization of quasipositive 3-braids implies that $m \geq 0$ or $r \geq -\lfloor \frac{3m-2}{2} \rfloor$ when $m < 0$. We note that this lower bound on r is not sharp but suffices for the purpose of this paper.

For the rest of the paper, when we use $\hat{\beta}$ to denote the smooth link given as the closure of a quasipositive 3-braid β , we assume that β is in the specific Garside normal form given by Equation 1.

2.2. Legendrian links in \mathbb{R}^3 . We briefly review the basic geometric terminology for Legendrian links in \mathbb{R}^3 that we will need for this paper. We refer readers to [Etn05] for an in-depth introduction to these materials. The standard contact structure ξ_{st} in \mathbb{R}^3 is the 2-plane field given by the kernel of the 1-form $\alpha_{st} = dz - ydx$. A link $\Lambda \subseteq (\mathbb{R}^3, \xi_{st})$ is **Legendrian** if it is everywhere tangent to ξ_{st} . In this paper, all Legendrian links are oriented and we consider Legendrian links up to Legendrian isotopy, i.e. ambient isotopy through a family of Legendrians.

We will often picture a Legendrian link via its front projection, namely the image of the link under the projection $\Pi_{xz} : \mathbb{R}^3 \rightarrow \mathbb{R}^2$ to the xz plane. There are two classical invariants associated to a Legendrian link. The **Thurston-Bennequin number** $\text{tb}(\Lambda)$ is the writhe of $\Pi_{xz}(\Lambda)$ minus the number of left (or right) cusps and the **rotation number** $\text{rot}(\Lambda)$ is given by $\frac{1}{2}(c_- - c_+)$ where c_-, c_+ are the number of cusps oriented downwards and upwards, respectively.

Any smooth link K has a Legendrian C^0 approximation. It follows from the Bennequin inequality that the Thurston-Bennequin number of a Legendrian representative of K is bounded above and we denote by $\overline{\text{tb}}(K)$ the maximum tb attained over all Legendrians of smooth link type K . Alternatively, the HOMFLY polynomial $P_K(v, z)$ also gives a bound on the classical invariants. In particular, for any Legendrian representative Λ of K , Fuchs and Tabachnikov showed in [FT97] that

$$\text{tb}(\Lambda) + |\text{rot}(\Lambda)| \leq -d_{P_K},$$

where d_{P_K} is the lowest degree in v of $P_K(v, z)$. Thus, $\overline{\text{tb}}(K) \leq -d_{P_K}$ and we refer this as the **HOMFLY bound** on the maximum Thurston-Bennequin number of K .



FIGURE 3. Local picture of stabilization.

Given a Legendrian link Λ , there is a local move that produces another Legendrian link in the same smooth knot type called stabilization and we describe it in the front diagram. First, the **stabilization** of Λ is obtained by removing a strand of Λ and replacing it with one of the zig-zags shown in Figure 3. Assuming Λ is oriented as shown, the left zig-zag gives a positive stabilization and the right one produces a negative stabilization, denoted by $S_+(\Lambda)$ and $S_-(\Lambda)$, respectively. One may check that $\text{tb}(S_\pm(\Lambda)) = \text{tb}(\Lambda) - 1$ and $\text{rot}(S_\pm(\Lambda)) = \text{rot}(\Lambda) \pm 1$. The **destabilization** of Λ is the reverse process of stabilization and may not always be possible for an arbitrary Legendrian.

Of particular interest in this paper are Legendrians obtained from the closure $\hat{\beta}$ of a 3-braid β , which we now describe using their front projections. Suppose $\hat{\beta}$ is presented by drawing β horizontally and joining the left and right ends of β by a nested set of non-intersecting arcs. We fix an orientation that goes counterclockwise around such a closure. If β is positive, a Legendrian representative of $\hat{\beta}$ is obtained by simply replacing all vertical tangencies with cusps; namely, the **rainbow closure** of β . See Figure 2 (left). [EV18, Theorem 3.4] proves that rainbow closures are the unique max-tb Legendrian representatives of braid positive links. Thus, observe from Figure 2 (left) that $\overline{\text{tb}}(\hat{\beta}) = |\beta| - 3$, where $|\beta|$ is the signed word length of β .

If in its Garside normal form, $\beta = \beta_+ \Delta^{-1}$, we isotope $\hat{\beta}$ to the (-1) -closure of $\beta_+ \Delta$ and replace all vertical tangencies with cusps; see Figure 2 (right). [CGG⁺25] shows that any Legendrian of this form is orientably fillable and is thus a max-tb Legendrian representative by Lemma 2.5 and Corollary 2.3. Observe from Figure 2 (right) that $\overline{\text{tb}}(\hat{\beta}) = |\beta|$.

Lastly, if $m < -1$, we isotope $\hat{\beta}$ to arrange one negative half twist vertically to the right of β_+ and the remaining $-m - 1$ negative half twists vertically to the left of β_+ . A replacement of all vertical tangencies with cusps yields a Legendrian representative of $\hat{\beta}$. We denote this Legendrian by $\Lambda_0(\beta)$ if m is even; see Figure 4 (left). Otherwise, we see a stabilization at the top of the front where we can immediately destabilize once to produce $\Lambda_0(\beta)$, pictured in Figure 4 (right). Note that $\text{tb}(\Lambda_0(\beta)) = |\beta| + \lfloor \frac{3m}{2} \rfloor$, and $\text{rot}(\Lambda_0(\beta)) = -\lfloor \frac{3(m+2)}{2} \rfloor$. In contrast with the cases $m \geq -1$ above, $\Lambda_0(\beta)$ is often not a max-tb representative. However, it will serve as an initial front that we iteratively destabilize in order to produce a (possibly non-unique) max-tb representative in Section 3.

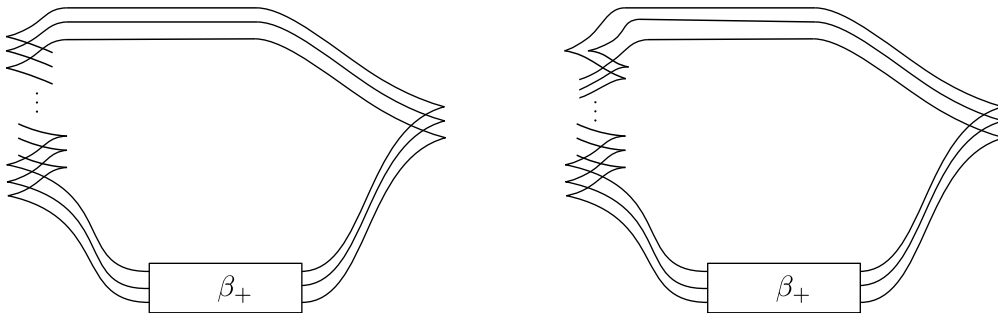


FIGURE 4. Initial fronts $\Lambda_0(\beta)$ for m even (left) and odd (right).

2.3. Rulings of Legendrian links. Normal rulings are combinatorial Legendrian invariants developed independently by Fuchs [Fuc03] and Chekanov–Pushkar [PC05]. They are intimately tied to augmentations of the Legendrian contact dg-algebra [Fuc03, FI04, Sab05, HR15], as well as the existence of exact Lagrangian fillings [Ati15, CCPR⁺23]. Here we define rulings and discuss some of their properties most relevant to fillability.

Given a Legendrian Λ with a fixed front projection D , a **normal ruling** $\rho(D)$ of Λ is a set of crossings $s(\rho)$ called **switches** such that resolving each of the switches yields a union of max-tb unknots $\Lambda_1, \dots, \Lambda_m$ satisfying

- each Λ_i has crossings, two cusps, and bounds an embedded disk
- exactly two link components are incident to any switches
- in a neighborhood of each switch, the incident ruling disks D_i are either completely nested or disjoint, as in the top row of Figure 5

A crossing with no switches is referred to as either a **departure** or **return** if it resembles the middle or bottom row, respectively, of Figure 5. We denote by $d(\rho)$ (resp. $r(\rho)$) the set of departures (resp. returns) of ρ .

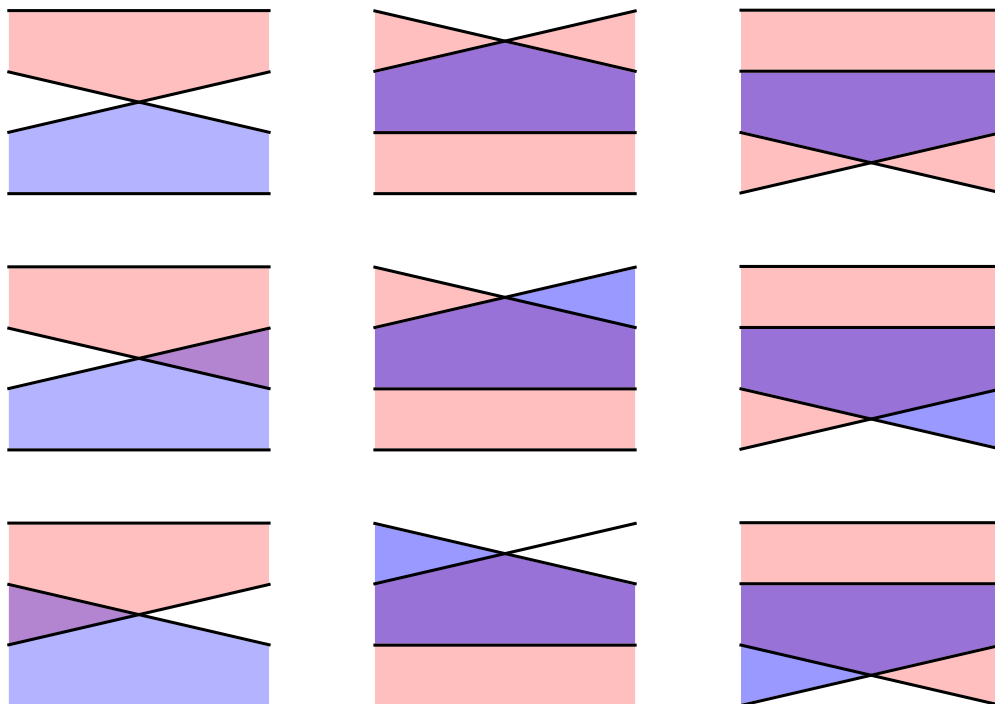


FIGURE 5. All possible configurations of ruling disks in a neighborhood of switches (top), departures (middle), and returns (bottom).

The set of rulings of D is a Legendrian isotopy invariant of Λ [PC05], hence we may discuss the rulings of Λ rather than the rulings of the front diagram D .

A normal ruling ρ is oriented if every switch of ρ occurs at a positive crossing, and unoriented otherwise. We define the **ruling polynomial** of Λ to be

$$R_{\Lambda}(z) = \sum_{\text{rulings } \rho} z^{s(\rho) - r(\rho) + 1}.$$

We define the **oriented ruling polynomial** $R_{\Lambda}^{\circ}(z)$ of Λ analogously by summing over all oriented rulings.

Given a smooth knot type K , normal rulings of its Legendrian representatives are closely related to various bounds on the maximum Thurston-Bennequin number of K .

Theorem 2.2 ([Rut06]). *Given a Legendrian link Λ of smooth knot type K ,*

- (1) the ruling polynomial $R_\Lambda(z)$ is the coefficient of $a^{-tb(\Lambda)-1}$ in the Kauffman polynomial $F_K(a, z)$.
- (2) the oriented ruling polynomial $R_\Lambda^\circ(z)$ is the coefficient of $a^{-tb(\Lambda)-1}$ in the HOMFLY polynomial $P_K(a, z)$.

Upper bounds on $tb(\Lambda)$ coming from the HOMFLY and Kauffmann polynomials then yield the following corollary.

Corollary 2.3 ([Rut06]). *A Legendrian link Λ admits a (n oriented) normal ruling if and only if the Kauffmann bound (resp. HOMFLY bound) on $tb(\Lambda)$ is sharp. Moreover, if Λ admits a normal ruling, it maximizes tb in its smooth isotopy class.*

2.4. Exact Lagrangian fillability. We end this section by a recollection of some results on exact Lagrangian cobordisms and fillings of a Legendrian link that we use in this paper. First, the symplectization $\text{Symp}(M, \ker(\alpha))$ of a contact manifold $(M, \ker(\alpha))$ is the symplectic manifold $(\mathbb{R}_t \times M, d(e^t \alpha))$. Given two Legendrian links $\Lambda_-, \Lambda_+ \subseteq (\mathbb{R}^3, \xi_{\text{st}})$, an **exact Lagrangian cobordism** $L \subseteq \text{Symp}(\mathbb{R}^3, \ker(\alpha_{\text{st}}))$ from Λ_- to Λ_+ is a cobordism Σ such that there exists some $T > 0$ satisfying the following:

- (1) $d(e^t \alpha_{\text{st}})|_\Sigma = 0$
- (2) $\Sigma \cap ((-\infty, T] \times \mathbb{R}^3) = (-\infty, T] \times \Lambda_-$
- (3) $\Sigma \cap ([T, \infty) \times \mathbb{R}^3) = [T, \infty) \times \Lambda_+$
- (4) $e^t \alpha_{\text{st}}|_\Sigma = df$ for some function $f : \Sigma \rightarrow \mathbb{R}$ that is constant on $(-\infty, T] \times \Lambda_-$ and $[T, \infty) \times \Lambda_+$.

An exact Lagrangian filling of the Legendrian link $\Lambda \subseteq (\mathbb{R}^3, \xi_{\text{st}})$ is an exact Lagrangian cobordism L from \emptyset to Λ that is embedded in $\text{Symp}(\mathbb{R}^3, \ker(\alpha_{\text{st}}))$. In this paper, we say that a Legendrian link is **orientably fillable** if it admits an orientable exact Lagrangian filling and a smooth knot type K is **orientably fillable** if it has an orientably fillable Legendrian representative. Similar terminology is defined for **non-orientable fillability**.

In the front projection, one can construct exact Lagrangian cobordisms via traces of Legendrian isotopies and the two additional elementary cobordisms given in Figure 6. Cobordisms constructed using these pieces are referred to as **decomposable**. We will also rely on a particular Lagrangian 1-handle attachment built out of several elementary exact Lagrangian cobordisms, as pictured in Figure 7. We refer to this cobordism as a **pinching cobordism**, as it is Hamiltonian isotopic, relative to the boundary, to the crossing resolution cobordism in the Lagrangian projection [Hug23a, Proposition 3.1].²

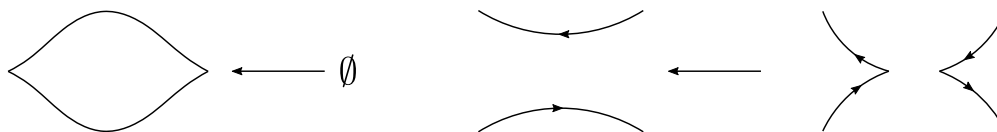


FIGURE 6. Minimum and (orientable) saddle cobordisms depicted in the front projection. The horizontal arrows point in the direction of expanding symplectic area.

Consider now a smooth knot type K obtained from the closure of a braid β . By constructing a filling explicitly from an oriented normal ruling in which all crossings are switched, Hayden-Sabloff proves the following result.

²This cobordism also appears in the literature as Lagrangian projection of the Legendrian lift of a generic perturbation of the D_4^- singularity in a Legendrian surface wavefront; See [Hug23a, Section 2.1.2] for more details.

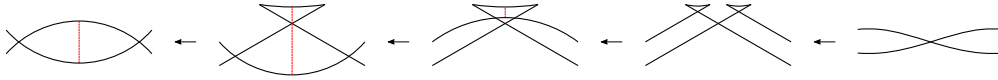


FIGURE 7. Pinching cobordism depicted in the front projection. The dashed red line depicts a contractible Reeb chord. The arrows point in the direction of expanding symplectic area.

Theorem 2.4 ([HS15], Theorem 1.1). *If β is positive, then K is orientably fillable.*

On the obstruction side, it is known that quasipositivity of β is a necessary condition for K to be fillable: a filling of K can be perturbed to a symplectic filling of a transverse knot [Eli95] and a smooth knot type with a symplectically fillable transverse representative is quasipositive [BO01].

Another notable obstruction of orientable fillability is the sharpness of HOMFLY bound on $\overline{\text{tb}}$. In particular, an orientable filling induces an augmentation of the Legendrian contact homology dg-algebra of Λ , which further produces an orientable ruling under the correspondence in [Fuc03, FI04, Sab05, Lev16]. The claimed obstruction is then a consequence of Corollary 2.3. In summary,

Lemma 2.5 ([HS15]). *If a Legendrian Λ is orientably fillable, then it is quasipositive and the HOMFLY bound on $\overline{\text{tb}}(K)$ is sharp.*

It is a conjecture of Hayden-Sabloff that these two necessary conditions together also give the sufficient condition for the orientable fillability of K . We shall consider their conjecture in the case when K is the closure of a 3-braid. In this context, Theorem 2.4 deals with the case when the integer m from Equation 1 is non-negative. When $m = -1$, the fact that K is orientably fillable follows from a general framework developed in [CGG⁺25]. In more detail, for $\beta \in \text{Br}_n^+$, the authors construct a graph encoding an (orientable) exact Lagrangian filling of the (-1) -closure of $\beta\Delta$, smoothly the braid closure of $\beta\Delta^{-1}$. One can produce a filling from this graph by applying the Legendrian weave construction of [CZ21, Section 2] to the graph after performing the minor modification discussed in [CN25, Definition 7.2].

We shall also consider non-orientable fillability of K . The case when K is positive is addressed in [CCPR⁺23].

Theorem 2.6 ([CCPR⁺23], Theorem 1.3). *If K is positive, it is not non-orientably decomposably fillable.*

The proof of this theorem makes use of the following ruling obstruction of non-orientable decomposable fillings, which we will also exploit in Section 5.

Lemma 2.7 ([CCPR⁺23], Corollary 3.8). *Let Λ be a Legendrian link with underlying smooth isotopy class K . If $R_\Lambda(z) = R_\Lambda^\circ(z)$, then no Legendrian representative of K admits a decomposable non-orientable fillings.*

3. MAX-TB REPRESENTATIVES OF QUASIPOSITIVE 3-BRAID CLOSURES

Before proving our main theorems, we produce a max-tb Legendrian representative $\Lambda_k(\beta)$ of $\hat{\beta}$ when $m \leq -2$. We will use these Legendrian representatives for obstructing orientable exact Lagrangian fillings of $\hat{\beta}$ when $m < -2$ and constructing non-orientable fillings when $m \leq -2$. Combined with previous results in the case $m \geq -1$ (c.f. Section 2.2), we shall prove Corollary 1.2 regarding the maximum Thurston-Bennequin number of quasipositive 3-braid links.

3.1. Constructing $\Lambda_k(\beta)$. Beginning with the Legendrian representative $\Lambda_0(\beta)$, introduced in Section 2.2, we give an iterative destabilization process to produce a sequence $\Lambda_0(\beta), \Lambda_1(\beta), \dots, \Lambda_k(\beta)$ that terminates in a max-tb representative $\Lambda_k(\beta)$ of $\hat{\beta}$ for $k = -\lfloor \frac{m+2}{2} \rfloor$. The key ingredient in this

process is a local smooth isotopy that we call a ZZS destabilization drawn in the bottom row of Figure 8. It involves an SZ move and a negative destabilization, which increases the tb of the link by 1 and decreases its rotation number by 3. In figures below, we indicate applications of ZZS destabilization by a red box.

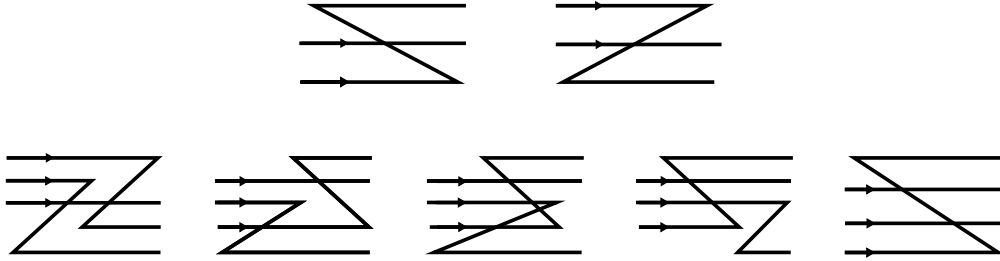


FIGURE 8. (Top) An SZ move. (Bottom) A ZZS destabilization, where the first step is an SZ move and the last step is a negative destabilization.

If $m = -2$, we maintain $\Lambda_0(\beta)$ with further modifications to come below. Otherwise, since $k_1 \geq 2$, we begin by rewriting β_+ as $\sigma_1^2 \beta_1$ for $\beta_1 = \sigma_1^{k_1-2} \sigma_2^{k_2} \dots \sigma_1^{k_{r-1}} \sigma_2^{k_r} \in \text{Br}_3^+$. We can then perform the sequence of isotopies and the ZZS destabilization pictured in the top row in Figure 9 followed by the isotopy pictured in Figure 10 (left) to produce $\Lambda_1(\beta)$. Note that in terms of the braid word, the isotopy in Figure 9 is equivalent to replacing $\Delta^{-2} \sigma_1^2$ by $\sigma_2^{-1} \sigma_1^{-2} \sigma_2^{-1}$. If $m = -3$ or -4 , we keep $\Lambda_1(\beta)$ with further modification to follow below. Otherwise, we continue destabilizing $\Lambda_i(\beta)$ in this manner, considering the following four cases at each step:

- (1) $\beta_i = \sigma_1^2 \beta_{i+1}$
- (2) $\beta_i = \sigma_2 \sigma_1^2 \beta_{i+1}$
- (3) $\beta_i = \sigma_2^2 \beta_{i+1}$
- (4) $\beta_i = \sigma_1 \sigma_2^2 \beta_{i+1}$

where $\beta_i \in \text{Br}_3^+$ for all $1 \leq i \leq k$. Since $k_i \geq 2$ for $1 \leq i \leq r-1$, these cases are exhaustive.

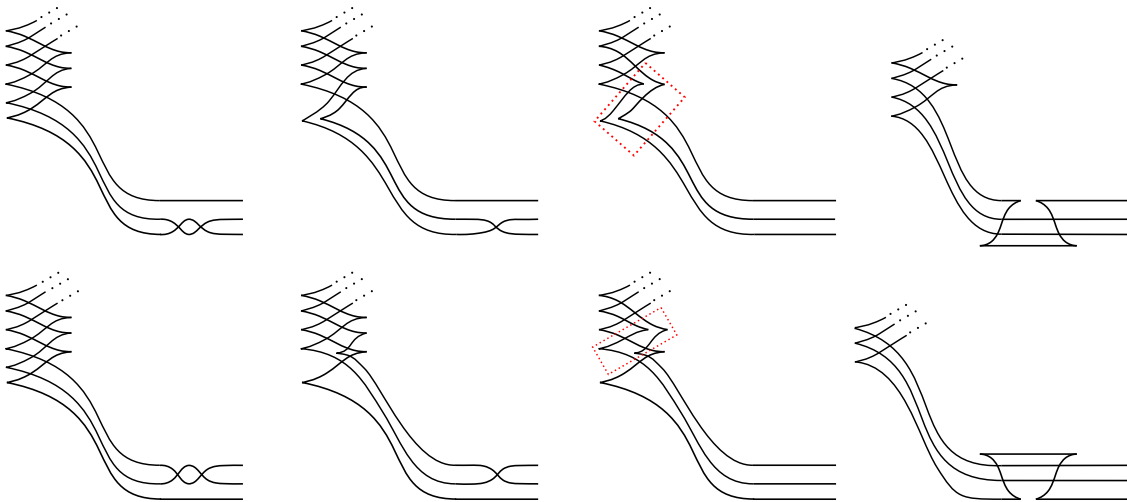


FIGURE 9. Destabilization of $\Lambda_i(\beta)$, $1 \leq i \leq k-1$ when β_i begins with either σ_1^2 or $\sigma_2 \sigma_1^2$ (top) or either σ_2^2 or $\sigma_1 \sigma_2^2$ (bottom).

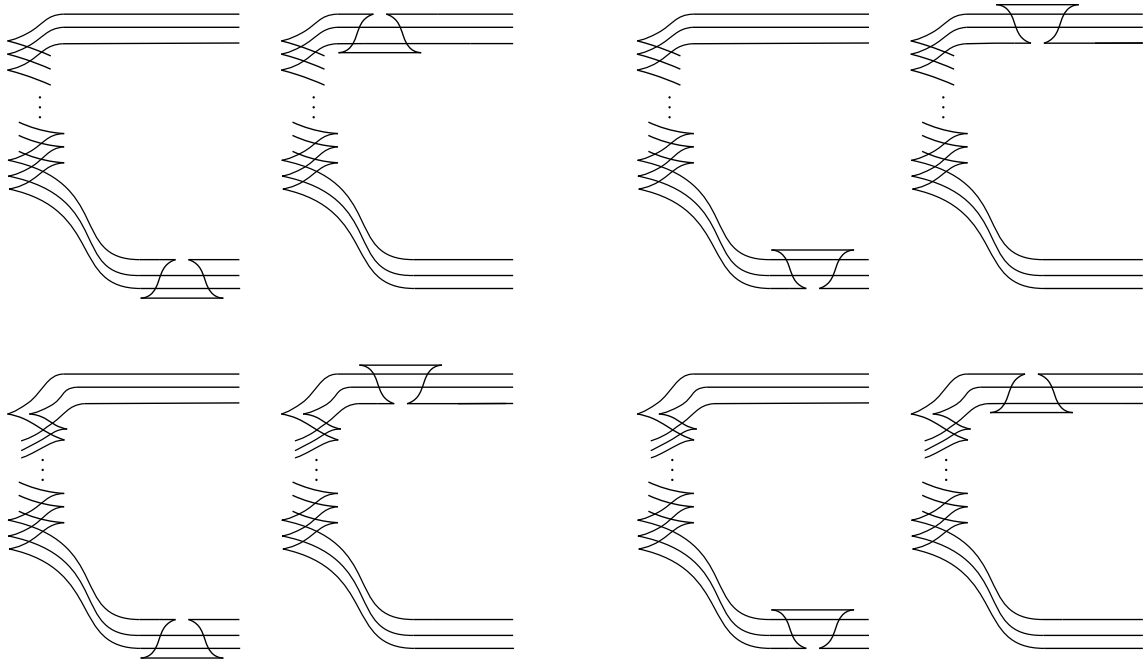


FIGURE 10. Legendrian isotopies performed after applying destabilization given in Figure 9 in Cases (1) (left) and (3) (right) when m is even (top) or m is odd (bottom).

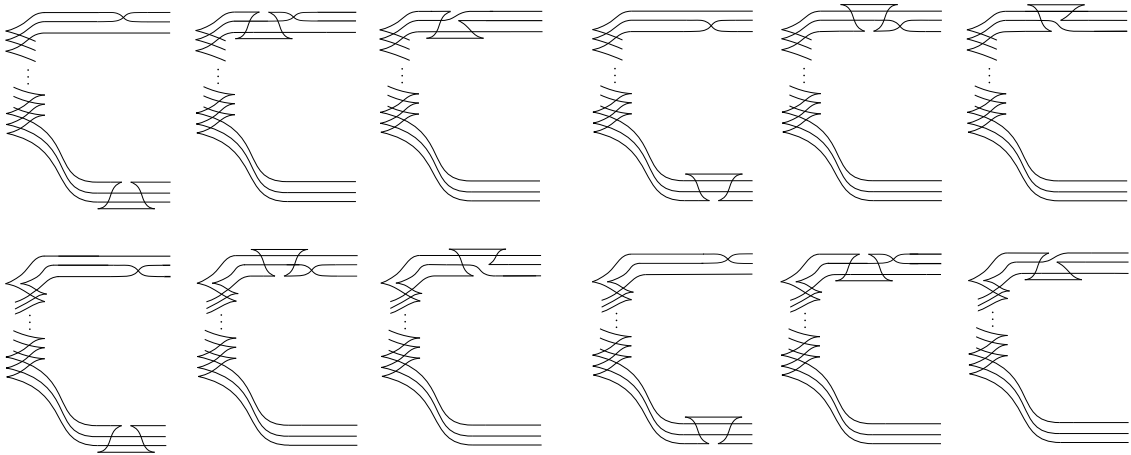


FIGURE 11. Legendrian isotopies performed after applying destabilization given in Figure 9 in Cases (2) (left) and (4) (right) when m is even (top) or m is odd (bottom).

In Case (1), we repeat the same destabilization procedure depicted in the top row of Figure 9 followed again by the isotopy from Figure 10 (left) to produce $\Lambda_{i+1}(\beta)$. In Case (2), we rotate the crossing σ_2 to the top of the front diagram, then perform the destabilization procedure depicted in the top row of Figure 9, followed by the isotopy from Figure 11 (left) to produce $\Lambda_{i+1}(\beta)$. Similarly, in Case (3), we perform the destabilization procedure depicted in the bottom row of Figure 9 followed by the isotopy from Figure 10 (right) to produce $\Lambda_{i+1}(\beta)$. In Case (4), we rotate the crossing σ_1 to the top of the front diagram, then perform the destabilization procedure depicted in the bottom row of Figure 9, followed by the isotopy from Figure 11 to produce $\Lambda_{i+1}(\beta)$.

If m is even, including $m = -2$, we can continue this process until we only have one negative half twist remaining on the left, resulting in $\Lambda_k(\beta)$. In particular, note that each destabilization reduces the number of negative half twists on the left by two. One can readily prove that $\Lambda_k(\beta)$ is a max-tb representative, but for the proof of Proposition 5.3 below, we perform an extra Reidemeister III move on the right closure of $\Lambda_k(\beta)$ as depicted in Figure 12 (left). This is made possible by the fact that $k_r \geq 2$ in this case. If β_{k-1} begins with σ_1^2 or $\sigma_2\sigma_1^2$, we perform another Reidemeister III move on the left closure of $\Lambda_k(\beta)$ as depicted in Figure 12 (center, right). We continue to denote the end result by $\Lambda_k(\beta)$.

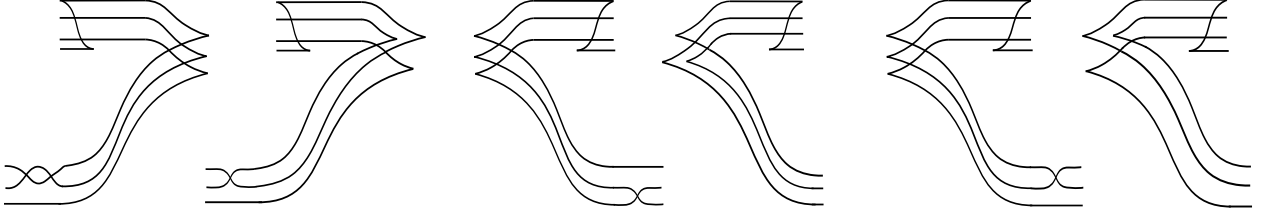


FIGURE 12. Reidemeister III moves performed for the case when m is even. It is done on the left closure only performed when β_k begins with either σ_1^3 or $\sigma_2\sigma_1^3$ (center) or $\sigma_1^2\sigma_2$ or $\sigma_2\sigma_1^2\sigma_2$ (right).

If m is odd, we iterate the process above to obtain $\Lambda_{k-1}(\beta)$ and treat the last iteration differently as follows. If $\Lambda_{k-1}(\beta)$ is of the form described in Case (1) or (2), we apply the destabilization procedure depicted in the top row of Figure 13. In Case (2), this is done after rotating the crossing σ_1 and we perform an additional Reidemeister II move depicted in Figure 14 (left) in the end. If $\Lambda_{k-1}(\beta)$ is of the form described in Case (3) or (4), we apply the destabilization procedure depicted in the bottom row of Figure 13. Again, in Case (4), this is done after rotating the crossing σ_1 and we perform an additional Reidemeister II move depicted in Figure 14 (right) in the end.

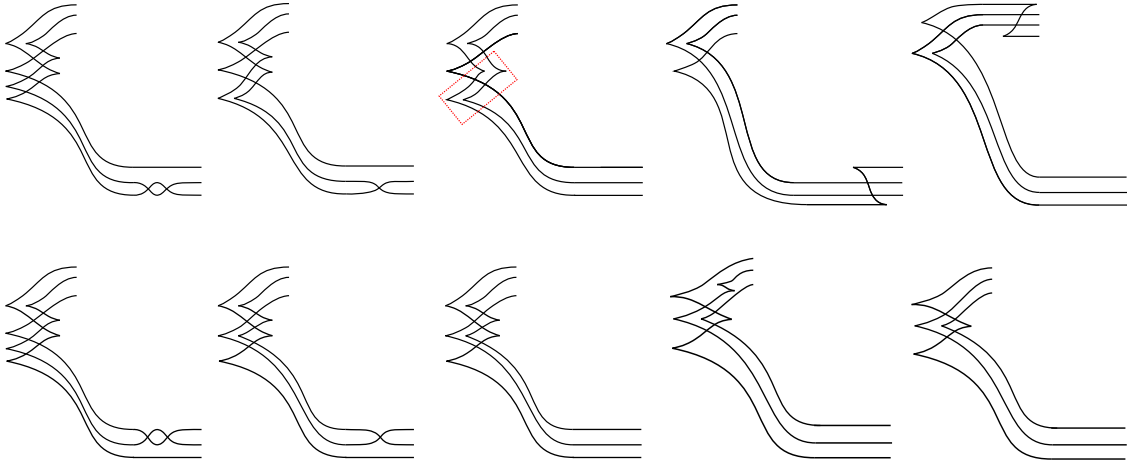


FIGURE 13. Destabilization of $\Lambda_{k-1}(\beta)$ when m is odd and β_{k-1} begins with σ_1^2 or $\sigma_2\sigma_1^2$ (top) and σ_2^2 or $\sigma_1\sigma_2^2$ (bottom).

At each step, since β is quasipositive, there are at least $|\Delta^{m-2i}| = 3(m-2i)$ crossings so that β_i is always of the form specified by one of Cases (1)-(4). The end result of this procedure is the Legendrian $\Lambda_k(\beta)$ with front projection given by the positive braid β_k and the pieces of the form

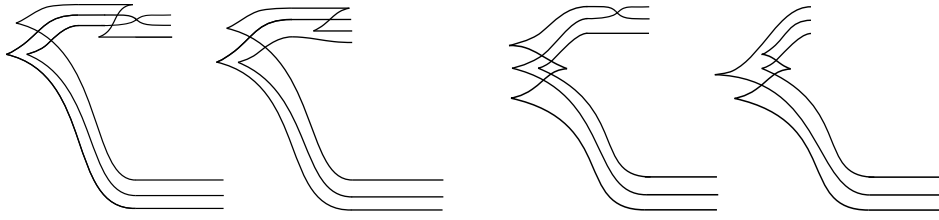


FIGURE 14. Reidemeister II moves performed for case when m is odd and β_{k-1} begins with a $\sigma_2\sigma_1^2$ (left) or $\sigma_1\sigma_2^2$ (right).

depicted in Figures 16, 17, or 18, and 19: the left and right closures, as well as a sequence of zigzags on the top. See Figure 15 for an example.

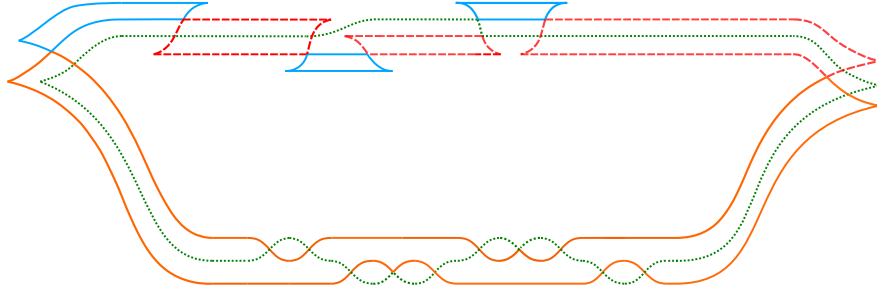


FIGURE 15. A ruling associated to $\Lambda_3(\sigma_1^3\sigma_2^2\sigma_1^2\sigma_2^2\sigma_1^3\sigma_2^3\sigma_1^2\Delta^{-7})$.

Note that, aside from the final destabilization when m is odd and β_{k-1} begins with σ_2^2 or $\sigma_1\sigma_2^2$, each destabilization is a ZZS move and thus decreases rotation number by 3. In consequence, we can compute that rotation number for our Legendrian representatives as

$$\text{rot}(\Lambda_k(\beta)) = - \left\lfloor \frac{3(m+2)}{2} \right\rfloor + 3 \left\lfloor \frac{m+4}{2} \right\rfloor - 1$$

when m is odd and $\beta_{k-1} = \sigma_2^2\beta_k$ or $\beta_{k-1} = \sigma_1\sigma_2^2\beta_k$, and

$$\text{rot}(\Lambda_k(\beta)) = - \left\lfloor \frac{3(m+2)}{2} \right\rfloor + 3 \left\lfloor \frac{m+2}{2} \right\rfloor$$

otherwise. This yields the following:

$$\begin{aligned} \text{tb}(\Lambda_k(\beta)) &= |\beta| + m - 1, \\ \text{rot}(\Lambda_k(\beta)) &= \begin{cases} 1 & m \text{ odd and } \beta_{k-1} = \sigma_2^2\beta_k \text{ or } \sigma_1\sigma_2^2\beta_k, \\ 0 & m \text{ even,} \\ -1 & \text{otherwise.} \end{cases} \end{aligned}$$

Pending our orientable fillability obstruction in Proposition 4.2 below, the computation of rotation number for m even and strictly less than -2 proves Corollary 1.3.

3.2. Constructing rulings of $\Lambda_k(\beta)$. We conclude this section by verifying that $\Lambda_k(\beta)$ is indeed a max-tb Legendrian representative of $\hat{\beta}$.

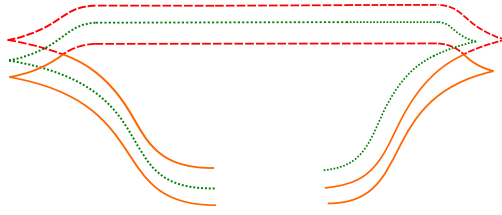


FIGURE 16. Ruling associated to the closure of $\Lambda_0(\beta)$ when $m = -2$.

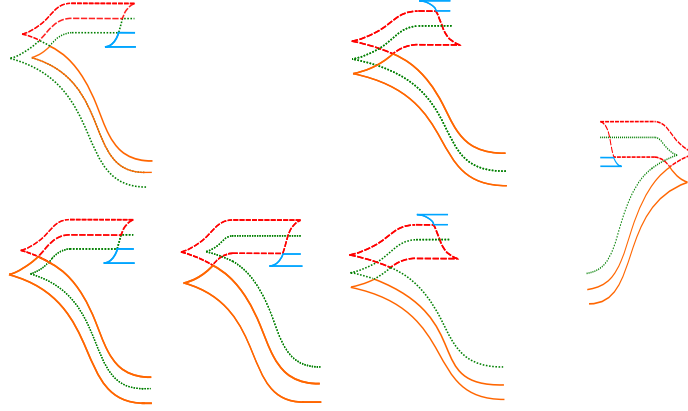


FIGURE 17. Rulings associated to the left and right closures of $\Lambda_k(\beta)$ when $m < -2$ is even. From left to right, the left closures correspond to cases when β_{k-1} begins with σ_1^3 or $\sigma_2\sigma_1^3$, $\sigma_1^2\sigma_2$ or $\sigma_2\sigma_1^2\sigma_2$, and σ_2^2 or $\sigma_1\sigma_2^2$. Rulings on the top (resp. bottom) row are used if β_k begins with σ_1 (resp. σ_2).

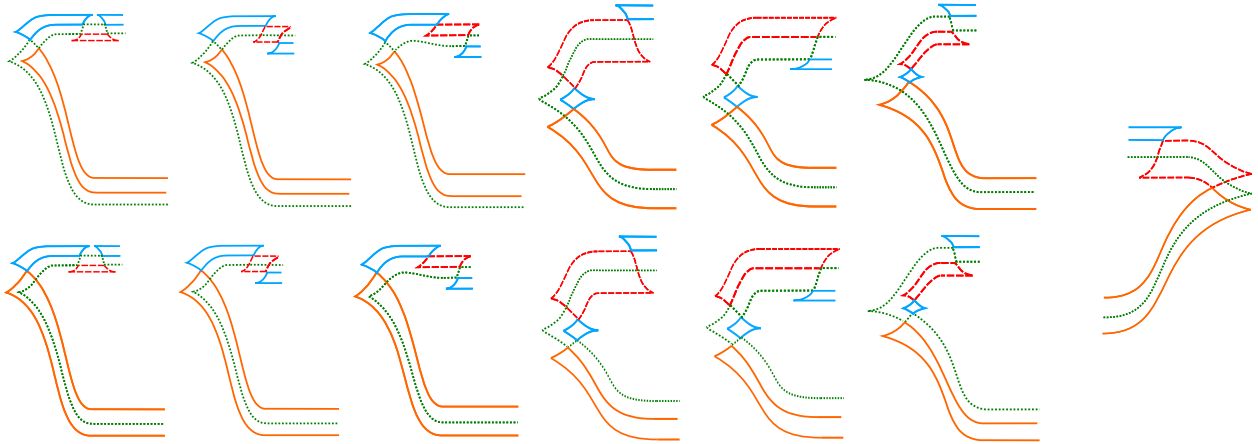


FIGURE 18. Rulings associated to the left and right closures of $\Lambda_k(\beta)$ when $m < -2$ is odd. From left to right, the left closures correspond to cases when β_{k-1} begins with σ_1^2 , $\sigma_2\sigma_1^2$, σ_2^2 , and $\sigma_1\sigma_2^2$, where the σ_1^2 , σ_2^2 cases are presented with two subcases. Rulings on the top (resp. bottom) row are used if β_k begins with σ_1 (resp. σ_2).

Proposition 3.1. For $m \leq -2$, $\Lambda_k(\beta)$ is a max-tb Legendrian representative of $\hat{\beta}$.

Proof. By Corollary 2.3, it suffices to show that $\Lambda_k(\beta)$ admits a normal ruling. Given that, by construction, $\Lambda_k(\beta)$ can be broken down into the pieces depicted in Figure 16, 18, 17, 19, and 20, we specify the ruling patterns locally in these figures and show that they glue without any conflicts. In particular, we use colors to indicate the boundary of the ruling disks and when two pieces of

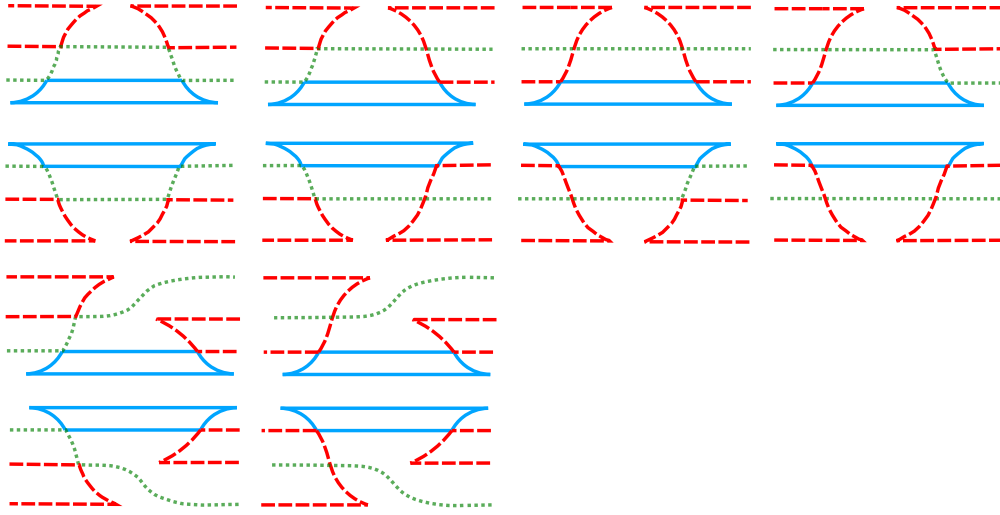


FIGURE 19. Rulings associated to the zigzag patterns on the top of $\Lambda_k(\beta)$. (From top to bottom) When m is even or odd, the zigzag patterns are obtained if β_i begins with σ_1^2 or σ_2^2 , σ_2^2 or σ_1^2 , $\sigma_2\sigma_1^2$ or $\sigma_1\sigma_2^2$, and $\sigma_1\sigma_2^2$ or $\sigma_2\sigma_1^2$. The last two columns only appear in the leftmost (k th) zigzag.

$\Lambda_k(\beta)$ are glued together, the colors of the overlapping strands ought to match with each other. The end result is a ruling consisting of a collection of thin disks on the top of $\Lambda_k(\beta)$ (in red and blue), a thin disk across the braid region of $\Lambda_k(\beta)$ (in orange), and a thick disk that goes around all regions of $\Lambda_k(\beta)$ (in green). See Figure 15 for an example.

For $m = -2$, we have $\Lambda_k(\beta) = \Lambda_0(\beta)$ and $\beta_k = \beta\sigma_2^{-1}$. The normal ruling is produced by gluing Figure 16 and the leftmost braid pattern on the second row of Figure 20 without any zigzags. By assumption, note that β_k begins with at least two σ_1 crossings. See below for a more detailed account of Figure 20.

Now, assume $m < -2$. We start by gluing the ruling on the top of $\Lambda_k(\beta)$ from right to left. The process largely follows the constructive recipe of $\Lambda_k(\beta)$ by scanning the word β from left to right. Begin with the right closure of $\Lambda_k(\beta)$ on which the ruling is depicted in Figure 17 when m is even and Figure 18 when m is odd. Since β begins with σ_1^2 , note that the first zigzag pattern attached to the right closure is determined to be on the top two rows of Figure 19. It is on the first (resp. second) row if m is even (resp. odd). Provided that Figure 17 or 18 fixes a ruling pattern on the right half of this zigzag, we choose the piece in the second column of Figure 19 to extend the ruling pattern leftwards.

The argument above falls under a general inductive paradigm as follows. For $i < k$, consider the i -th zigzag pattern obtained from β_{i-1} and fix a ruling pattern on its right half that can be found in Figure 19. Our goal is to complete this ruling pattern by choosing one in Figure 19 and extend it to the right half of the $(i+1)$ -th zigzag. We consider the four cases of β_{i-1} outlined before. In Case (1), the i -th zigzag pattern is on the top two rows of Figure 19. It is on the first (resp. second) row if m is even (resp. odd). We choose the unique piece in the first two columns that completes the fixed ruling pattern. Since $k_1, \dots, k_r \geq 2$, note that β_i cannot begin with $\sigma_2\sigma_1^2$ and the ruling pattern extends uniquely to the right half of the $(i+1)$ -th zigzag that can be found in Figure 19. Case (3) is completely similar. In this case, note that β_i cannot begin with $\sigma_1\sigma_2^2$ and the ruling pattern extends uniquely. In Case (2), the i -th zigzag pattern is in the bottom two rows of Figure 19. It is in the third (resp. fourth) row if m is even (resp. odd). The fixed ruling pattern is the same on the right half of the two candidates. If β_i begins with σ_1^2 or $\sigma_1\sigma_2^2$ (resp. σ_2^2), we choose the ruling pattern on the left (resp. right) and it extends uniquely to the right half of the $(i+1)$ -th zigzag; β_i cannot begin with $\sigma_2\sigma_1^2$. Case (4) is completely similar to Case (2) in the sense

of Case (3) being similar to Case (1). Throughout this process, note that we have only used the first two columns of Figure 19.

Proceeding inductively, we obtain a ruling pattern on the right half of the k -th zigzag among the ones depicted in Figure 19. In the mean time, Figure 17 or 18 fixes a ruling pattern on the left half of the k -th zigzag. For the left closures with two ruling patterns presented, we choose the one on top if β_k begins with σ_1 and the one on bottom otherwise. Note that when m is even and β_{k-1} begins with $\sigma_1^2\sigma_2$ or $\sigma_2\sigma_1^2\sigma_2$, β_k necessarily begins with σ_2 . By inspection, we see that the left closures extend the ruling pattern on the right half of the k -th zigzag in all cases without any conflicts. The resulting ruling pattern on the k -th zigzag is among those depicted in Figure 19.

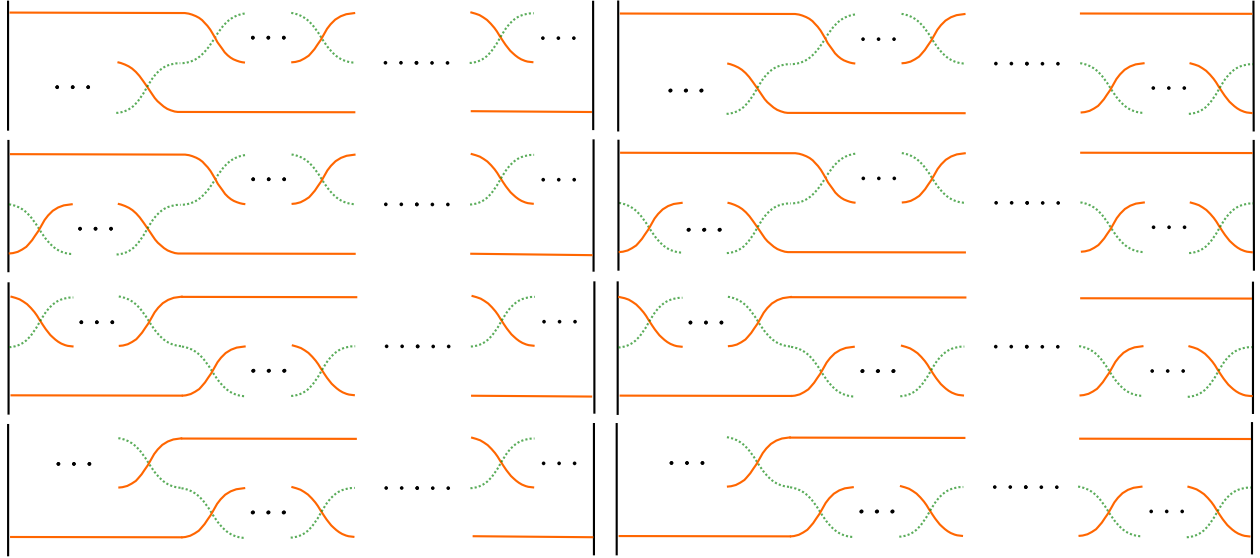


FIGURE 20. Rulings associated to the braid region of $\Lambda_k(\beta)$ when m is even (left) and odd (right). The ellipses within each block $\sigma_i^{k_i}$ indicate switches.

It remains to fit a ruling pattern of the braid region β_k into the picture. Such a pattern is given in Figure 20 for all possible configurations of β_k , consisting of only a green path and an orange path. Unless otherwise stated in the figure, in each block $\sigma_i^{k_i}$ of β_k , all crossings except the first and the last ones are switches indicated by an ellipse. However, note that the first and last block of β_k may begin or end with a number of switches respectively. Again, an inspection verifies that the ruling patterns agree with those on the closures in Figure 17 or 18 in all cases. In particular, when the green path enters (resp. exists) in the middle of the two orange paths, we are ensured that the first (resp. last) block of β_k contains at least two crossings.

In summary, we obtain a collection of embedded disks with boundary on $\Lambda_k(\beta)$, as claimed above. Further, all switches are disjoint except those at σ_2 crossings in the middle of β_k , which are nested. Thus, we obtain a normal ruling of $\Lambda_k(\beta)$ and by Corollary 2.3, this proves that $\Lambda_k(\beta)$ is a max-tb representative of its smooth link type $\hat{\beta}$. \square

4. ORIENTABLE FILLABILITY OF 3-BRAID CLOSURES

We are now ready to discuss exact Lagrangian fillability of (quasipositive) 3-braid closures $\hat{\beta}$. In this section, we complete the proof of Theorem 1.1 by showing that $\hat{\beta}$ is orientably fillable if $m = -2$ and not if $m < -2$. We begin with the construction of orientable fillings.

Proposition 4.1. $\hat{\beta}$ is orientably exact Lagrangian fillable if $m = -2$.

Proof. It suffices to construct an orientable exact Lagrangian filling of $\Lambda_0(\beta)$. In the notation of Equation 1, note that according to Orevkov's criterion of quasipositivity, $r \geq 4$. First, observe that when $\beta = \sigma_1^2 \sigma_2^2 \sigma_1^2 \sigma_2^2 \Delta^{-2}$, the Legendrian $\Lambda_0(\beta)$ admits an exact Lagrangian filling. This observation can be verified by pinching the fourth and eighth crossings of β and applying a braid move to obtain $\Lambda_0(\Delta^2 \Delta^{-2})$, which is isotopic to three unlinked max-tb Legendrian unknots. The claim then follows from observing that any $\Lambda_0(\beta)$ of the form given in the statement of the lemma is exact Lagrangian cobordant to $\Lambda_0(\sigma_1^2 \sigma_2^2 \sigma_1^2 \sigma_2^2 \Delta^{-2})$ when $r \geq 4$. We can produce an exact Lagrangian cobordism by first pinching a subset of the first $k_1 + k_2 + k_3 + k_4$ crossings to obtain the braid $\sigma_1 \sigma_1 \sigma_2 \sigma_1 \sigma_1 \sigma_2 \sigma_1^{k_5} \dots \sigma_2^{k_r}$. We then perform a sequence of Reidemeister III moves and pinches to eliminate the remaining $k_5 + \dots + k_r$ crossings. Concatenating this cobordism with the filling of $\Lambda(\sigma_1 \sigma_1 \sigma_2 \sigma_1 \sigma_1 \sigma_2)$ yields a filling of $\Lambda_0(\beta)$, as desired. \square

Next, we turn to the obstructive part of Theorem 1.1, namely,

Proposition 4.2. $\hat{\beta}$ is not orientably exact Lagrangian fillable if $m < -2$.

Proof. Using the max-tb Legendrian representatives $\Lambda_k(\beta)$ of $\hat{\beta}$ found in Section 3, we prove explicitly that the HOMFLY bound on $\overline{\text{tb}}(\hat{\beta})$ is not sharp, which obstructs orientable fillability by Lemma 2.5. Recall from our earlier computations in Section 2.2 and Section 3 that

$$\begin{aligned} \text{tb}(\Lambda_k(\beta)) - \text{tb}(\Lambda_0(\beta)) &= - \left\lfloor \frac{m+2}{2} \right\rfloor, \\ |\text{rot}(\Lambda_k(\beta))| - |\text{rot}(\Lambda_0(\beta))| &\leq 3 \left\lfloor \frac{m+2}{2} \right\rfloor, \end{aligned}$$

Thus, for $m < -2$,

$$\overline{\text{tb}}(\hat{\beta}) = \text{tb}(\Lambda_k(\beta)) \leq \text{tb}(\Lambda_k(\beta)) + |\text{rot}(\Lambda_k(\beta))| < \text{tb}(\Lambda_0(\beta)) + |\text{rot}(\Lambda_0(\beta))| \leq d_{PK},$$

and the HOMFLY bound on $\overline{\text{tb}}(\hat{\beta})$ is not sharp, as desired. \square

Remark 4.3. Rather than computing the HOMFLY bound directly, one could also observe that for $m < -2$, the Legendrian $\Lambda_k(\beta)$ admits no orientable rulings as each ruling must have a switch at at least one of the negative crossings in the left or right closure. The desired result then follows from the fact that orientably fillable Legendrian links must admit an orientable ruling.

We conclude this section by a comment about our orientable filling construction from the Legendrian weave perspective, which we then use to conclude Corollary 1.7. We refer readers to [CZ21, Section 2] for necessary preliminaries on Legendrian weaves.

Corollary 4.4. $\Lambda_0(\beta \Delta^m)$ admits an exact Lagrangian filling obtained as the Lagrangian projection of a Legendrian weave for all $m \geq -2$.

Proof. The exact Lagrangian fillings of Proposition 4.1 are constructed by using braid isotopies and pinching cobordisms to produce an orientable exact Lagrangian cobordism to the unlink. In the language of [CZ21, Section 2], these braid isotopies correspond to hexavalent vertices, while the pinching cobordisms correspond to trivalent vertices. For $m \geq -1$, the orientable exact Lagrangian fillings of [CGG⁺25] discussed in Subsection 2.4 are constructed as the Lagrangian projection of Legendrian weaves. \square

5. NON-ORIENTABLE FILLABILITY OF QUASIPOSITIVE 3-BRAID CLOSURES

In this section, we characterize non-orientable fillability of quasipositive 3-braid closures, proving Theorem 1.8. First, we extend Theorem 2.6 from braid positive Legendrians to the case of $m = -1$ and prove the obstructive part of Theorem 1.8. We do so following the proof technique in [CCPR⁺23], namely showing that every normal ruling of $\Lambda_0(\beta)$ is orientable.

Lemma 5.1. *Every normal ruling of $\Lambda_0(\beta_+\Delta^{-1})$ is orientable.*

Proof. $\Lambda_0(\beta_+\Delta^{-1})$ has one negative half twist on the right of the front diagram and no negative crossings on the left. This guarantees that all of the ruling disks must be thick disks passing through both the top and bottom set of strands of the front projection. Therefore, any ruling disk of $\Lambda_0(\beta_+\Delta^{-1})$ with negative switches must switch at exactly two negative crossings. By inspection, one can verify that there are no such rulings, as any possible candidates must have illegally nested disks at switched crossings. \square

Note that the above result and method of proof hold for braid index greater than three as well.

Proposition 5.2. *$\hat{\beta}$ is not non-orientably decomposably fillable if $m = -1$.*

Proof. This follows immediately from Lemma 5.1 and Lemma 2.7. \square

Finally, we construct a non-orientable exact Lagrangian filling of $\hat{\beta}$ for $m \leq -2$.

Proposition 5.3. *$\hat{\beta}$ is non-orientably fillable if $m \leq -2$.*

Proof. We prove the statement above by showing that the ruling constructed in the proof of Proposition 3.1 is induced by a non-orientable filling. Specifically, we claim that the switches in the ruling can all be resolved via the pinching cobordism depicted in Figure 7 or, in the presence of a cusp, by first performing a Reidemeister II move, as in Figure 21 and then applying the local move from Figure 7.

We first verify the claim for $m = -2$. In this case, recall that the ruling of $\Lambda_{k=0}(\beta)$ is given by combining Figure 16 with the braid region depicted in the first column, second row of Figure 20. To resolve the switched crossings, we start with the rightmost switch of Figure 16, and resolve it via a horizontal reflection of Figures 21 and 7. This then allows us to resolve all of the switches in the braid region again starting with the rightmost, freely performing Reidemeister II moves with the orange strands as needed. After resolving all of these switches, we can perform one more Reidemeister II move to make the green and orange ruling disks disjoint, allowing us to resolve the switch between the red and orange ruling disks on the left of Figure 20. This yields three unlinked unknots, which we can then fill in with disks to produce an exact Lagrangian filling of $\Lambda_k(\beta)$.

Our claim can be verified for $m < -2$ by an inspection of the local pieces of rulings depicted in Figures 17, 18, 19, and 20. In particular, we see that during the construction of the ruling in the proof of Proposition 3.1, the red and blue thin ruling disks are either disjoint from the rest of the front after resolving the switches, or they can be made disjoint after performing a single Reidemeister II move to pull them away from the green strand. Note that we require gluing of zig-zag patterns exactly as specified in the proof, as otherwise we might have the green strand non-trivially linked with one of the red or blue thin disks. Likewise, when we examine the green and orange disks of the ruling, we can produce a pair of max-tb unknots by a sequence of Reidemeister II moves and crossing resolutions, as in the $m = -2$ case. In particular, the ruling patterns in Figure 20 where the first crossing of β is switched are matched with ruling patterns from Figures 17 and 18 that force the corresponding ruling disks to be disjoint at the first crossing of β .

To produce an exact Lagrangian filling inducing the ruling described in the proof of Proposition 3.1, we start scanning the front left to right and performing pinching cobordisms at each of the

switched crossings as they appear, freely applying the isotopy from Figure 21 to facilitate this. The one obstruction to this particular ordering of pinching cobordisms that we encounter is when, in the zigzag patterns at the top of the front, a red ruling disk has a green strand passing through it. The red and green ruling disks are unlinked, but we cannot isotope them to be disjoint without first resolving one of the switched crossings of the red disk. When the red disk appears in a position similar to the leftmost red disk in Figure 15 or its vertical reflection, we instead perform the pinching cobordism at the other switched crossing involving the red disk. We then isotope the red disk to be disjoint from the green, and performing a pinching cobordism at the remaining switched crossing involving the red disk. When resolving the switched crossings in β , we freely perform Reidemeister II moves as before. Direct inspection of the rulings associated to the left and right closures as pictured in Figure 17 and 18 verifies that we can perform a similar process there as well. The end result of this process is a collection of unlinked max-tb unknots, which we can fill in with the minimum cobordism pictured in Figure 6 (left) to produce a non-orientable exact Lagrangian filling of $\Lambda_k(\beta)$. \square

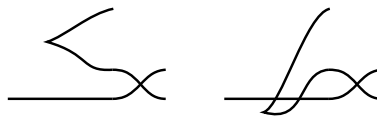


FIGURE 21. Preparatory isotopy before performing a pinching cobordism.

REFERENCES

- [ABL22] Byung Hee An, Youngjin Bae, and Eunjeong Lee. Lagrangian fillings for Legendrian links of finite or affine Dynkin type, 2022. arxiv:2201.00208.
- [Ati15] Watchareean Atiponrat. An obstruction to decomposable exact Lagrangian fillings, 2015.
- [BO01] Michel Boileau and Stepan Orevkov. Quasi-positivité d’une courbe analytique dans une boule pseudoconvexe. *C. R. Acad. Sci. Paris Sér. I Math.*, 332(9):825–830, 2001.
- [BST15] Frédéric Bourgeois, Joshua M. Sabloff, and Lisa Traynor. Lagrangian cobordisms via generating families: construction and geography. *Algebr. Geom. Topol.*, 15(4):2439–2477, 2015.
- [CCPR⁺23] Linyi Chen, Grant Crider-Phillips, Braeden Reinoso, Joshua M. Sabloff, and Leyu Yau. Non-orientable Lagrangian fillings of Legendrian knots. *Mathematical Proceedings of the Cambridge Philosophical Society*, 176(1):123–153, 2023.
- [CG22] Roger Casals and Honghao Gao. Infinitely many Lagrangian fillings. *Ann. of Math. (2)*, 195(1):207–249, 2022.
- [CG24] Roger Casals and Honghao Gao. A Lagrangian filling for every cluster seed. *Invent. Math.*, 237(2):809–868, 2024.
- [CGG⁺25] Roger Casals, Eugene Gorsky, Mikhail Gorsky, Ian Le, Linhui Shen, and José Simental. Cluster structures on braid varieties. *J. Amer. Math. Soc.*, 38(2):369–479, 2025.
- [Cha10] Baptiste Chantraine. Lagrangian concordance of Legendrian knots. *Algebr. Geom. Topol.*, 10(1):63–85, 2010.
- [CN22] Roger Casals and Lenhard Ng. Braid loops with infinite monodromy on the Legendrian contact DGA. *J. Topol.*, 15(4):1927–2016, 2022.
- [CN25] Roger Casals and Yoon Jae Nho. Spectral networks and Betti Lagrangians, 2025.
- [CSC23] Orsola Capovilla-Searle and Roger Casals. On Newton polytopes of Lagrangian augmentations, 2023.
- [CSHW25] Orsola Capovilla-Searle, James Hughes, and Daping Weng. Augmentations, fillings, and clusters for 2-bridge links. *Selecta Math. (to appear)*, 2025.
- [CW22] Roger Casals and Daping Weng. Microlocal theory of Legendrian links and cluster algebras. arxiv:2204.13244, 2022.
- [CZ21] Roger Casals and Eric Zaslow. Legendrian weaves. *Geom. Topol.*, 2021.
- [EHK16] Tobias Ekholm, Ko Honda, and Tamás Kálmán. Legendrian knots and exact Lagrangian cobordisms. *J. Eur. Math. Soc. (JEMS)*, 18(11):2627–2689, 2016.
- [Eli95] Y. Eliashberg. Topology of 2-knots in \mathbf{R}^4 and symplectic geometry. In *The Floer memorial volume*, volume 133 of *Progr. Math.*, pages 335–353. Birkhäuser, Basel, 1995.
- [Etn05] John B. Etnyre. Legendrian and transversal knots. In *Handbook of knot theory*, pages 105–185. Elsevier B. V., Amsterdam, 2005.

- [EV18] John Etnyre and Vera Vértesi. Legendrian satellites. *Int. Math. Res. Not. IMRN*, (23):7241–7304, 2018.
- [FI04] Dmitry Fuchs and Tigran Ishkhanov. Invariants of Legendrian knots and decompositions of front diagrams. *Mosc. Math. J.*, 4(3):707–717, 783, 2004.
- [FT97] Dmitry Fuchs and Serge Tabachnikov. Invariants of Legendrian and transverse knots in the standard contact space. *Topology*, 36(5):1025–1053, 1997.
- [Fuc03] Dmitry Fuchs. Chekanov–Eliashberg invariant of Legendrian knots: existence of augmentations. *J. Geom. Phys.*, 47(1):43–65, 2003.
- [Hed] Matthew Hedden. Notions of positivity and the Ozsváth–Szabó concordance invariant. arXiv:math/0509499v1.
- [HR15] Michael B. Henry and Dan Rutherford. Ruling polynomials and augmentations over finite fields. *J. Topol.*, 8(1):1–37, 2015.
- [HS15] Kyle Hayden and Joshua M. Sabloff. Positive knots and Lagrangian fillability. *Proc. Amer. Math. Soc.*, 143(4):1813–1821, 2015.
- [Hug23a] James Hughes. Lagrangian fillings in A -type and their Kálmán loop orbits. *Rev. Mat. Iberoam.*, 39(5):1681–1723, 2023.
- [Hug23b] James Hughes. Weave-realizability for D -type. *Algebr. Geom. Topol.*, 23(6):2735–2776, 2023.
- [Lev16] C. Levenson. Augmentations and rulings of Legendrian knots. *J. Symplectic Geom.*, 14(4):1089–1143, 2016.
- [LM25] Charles Livingston and Allison H. Moore. Knotinfo: Table of knot invariants. URL: knotinfo.org, July 2025.
- [LN24] Robert Lipshitz and Lenhard Ng. Torsion in linearized contact homology for Legendrian knots. *Michigan Math J. (to appear)*, 2024.
- [LS19] Erin R. Lipman and Joshua M. Sabloff. Lagrangian fillings of Legendrian 4-plat knots. *Geom. Dedicata*, 198:35–55, 2019.
- [Ore04] Stepan Yu. Orevkov. Quasipositivity problem for 3-braids. *Turkish J. Math.*, 28(1):89–93, 2004.
- [Ore15] Stepan Yu. Orevkov. Algorithmic recognition of quasipositive 4-braids of algebraic length three. *Groups Complex. Cryptol.*, 7(2):157–173, 2015.
- [Pan17] Yu Pan. Exact Lagrangian fillings of Legendrian $(2, n)$ torus links. *Pacific J. Math.*, 289(2):417–441, 2017.
- [PC05] P. E. Pushkar' and Yu. V. Chekanov. Combinatorics of fronts of Legendrian links, and Arnold's 4-conjectures. *Uspekhi Mat. Nauk*, 60(1(361)):99–154, 2005.
- [Rut06] Dan Rutherford. Thurston–Bennequin number, Kauffman polynomial, and ruling invariants of a Legendrian link: the Fuchs conjecture and beyond. *Int. Math. Res. Not.*, pages Art. ID 78591, 15, 2006.
- [Sab05] Joshua M. Sabloff. Augmentations and rulings of Legendrian knots. *Int. Math. Res. Not.*, (19):1157–1180, 2005.
- [STWZ19] Vivek Shende, David Treumann, Harold Williams, and Eric Zaslow. Cluster varieties from Legendrian knots. *Duke Math. J.*, 168(15):2801–2871, 2019.
- [STZ17] Vivek Shende, David Treumann, and Eric Zaslow. Legendrian knots and constructible sheaves. *Invent. Math.*, 207(3):1031–1133, 2017.
- [Tag19] Keiji Tagami. On the Lagrangian fillability of almost positive links. *J. Korean Math. Soc.*, 56(3):789–804, 2019.
- [TZ18] David Treumann and Eric Zaslow. Cubic planar graphs and Legendrian surface theory. *Adv. Theor. Math. Phys.*, 22(5):1289–1345, 2018.

DUKE UNIVERSITY, DEPT. OF MATHEMATICS, DURHAM, NC 27708, USA

Email address: james.hughes@duke.edu

DUKE UNIVERSITY, DEPT. OF MATHEMATICS, DURHAM, NC 27708, USA

Email address: jason.ma@duke.edu